JNEST EISSN: 2961-8738 ● PISSN: 2961-8916 ● DOI: 10.56741/jnest.v5i03.2446
Article Received 23 June 2026, Revised 6 October 2026

Improved Perturb and Observe Algorithm for Residence Time in the Oxygen Concentrator System

Shalma N. Hida, Asep Suhendi*, and Muhammad Z. Romdlony

***Abstract*—The oxygen demand has been increasing lately. Consequently, high-purity oxygen must be generated by oxygen concentrators. Because of its high efficiency and low operating costs, pressure swing adsorption is the most efficient method utilized in oxygen concentrator systems. In practical applications, this method necessitates multiple trials to determine the cycle time that produces the maximum oxygen concentration, with the system requiring to be stopped in advance. The use of this equipment supports the automation of the perturb and observe approach by enabling the cycle time to be changed without interrupting the system. This algorithm does nevertheless face the usual problem in that it may result in local maximums that restrict the search for the global maximum. This implies that modifications to the algorithm are required. The cycle time step size is changed to improve the P&O modification. Initially, a larger step size is employed, and if a crossing path in the produced oxygen concentration is found, the step size will be reduced. The experiment's findings demonstrate that P&O modifications might assist oxygen concentrator systems in avoiding local maximum problems as well as supply high-purity oxygen to fulfil oxygen needs.**

***Index Terms*—Cycle time, Oxygen Concentrators, Perturb and Observe Algorithm, Pressure Swing Adsorption, Purity Oxygen.**

I. Introduction

The global health and economic conditions have been severely impacted by the COVID-19 epidemic. These conditions lower oxygen intake and may even cause organ failure. Because less than 92% is the recommended oxygen saturation target by the World Health Organization, medical attention in the form of oxygen supplementation is necessary [1]. Oxygen concentrators are medical equipment that treat breathing-related disorders or conditions by delivering oxygen to patients whose blood oxygen content is below normal. Pressure swing adsorption (PSA), air separation units, integrated energy systems, ion transport membranes, and other techniques are some methods to raise oxygen levels [2]. The PSA process is considered a cost-effective technology for oxygen generation because of its relatively low energy consumption, simple operation, compact equipment requirements, and low operating and management costs. These advantages make PSA particularly suitable for small- and medium-scale installations and decentralized oxygen generation [3]. In the process, PSA pays attention to pressure as a variable that affects the purity of the oxygen produced. This is related to the length of the air supply line inserted into the chamber, which affects the pressure within the chamber [2]. But in addition, the duration of the air-adsorbent surface interaction can also have an impact on the adsorbent's effectiveness [4].

Studies are needed to find the best cycle times for PSA's oxygen-generating process. Usually, it takes several tries to get this value. Therefore, a system for automated control that can assist in determining the ideal cycle time value is required. The perturb and observe algorithm (P&O) is one of them. Since the purpose of P&O in an MPPT PV system is to find the maximum power value by changing the supply voltage, similar to an oxygen concentrator system. That is to find the maximum oxygen concentration value by changing the cycle time applied. Also consider the output patterns of the P&O algorithm on MPPT PV systems are similar with the output of oxygen concentrator, it seems sense that oxygen concentrator systems might also use it for control [5]. One problem with using the P&O algorithm in practice is that because the maximum locality exists, the process becomes looped at the maximum local point and cannot go to the maximum global point. To avoid this, modifications were made to the P&O algorithm [6].

From the explanation above, the development process is needed in creating a system that can produce high oxygen purity with the most efficient method, namely pressure swing adsorption and automation control by implementing the perturb and observe algorithm on the oxygen concentrator system.

II. Related Works

A. Previous Research

Previous studies have investigated various oxygen production methods and reported that oxygen concentrators offer advantages in terms of safety, cost, size, and efficiency [7]–[8]. Among these technologies, pressure swing adsorption (PSA) is a well-established gas separation process due to its compact equipment, low energy consumption, relatively low capital cost, operational safety, and simplicity, making it suitable for small-scale applications [3]. The effects of cycle time and operating conditions on oxygen concentration have also been investigated in previous studies [5], [9].

To the best of the authors' knowledge, the perturb and observe (P&O) algorithm has not yet been applied to optimize oxygen concentration in a PSA-based oxygen concentrator. The P&O algorithm is widely used in maximum power point tracking (MPPT) for photovoltaic systems, where the operating point is iteratively adjusted to achieve the maximum output [10]. However, conventional P&O algorithms may become trapped around a local maximum under certain operating conditions. Adaptive step-size strategies have therefore been proposed to improve the search for the global maximum by reducing the step size when the

Shalma Nur Hida, **Asep Suhendi** (Corresponding Author), and **Muhammad Zakiyullah Romdlony** are with the School of Electrical Engineering, Telkom University, Bandung, Indonesia. Corresponding Author Email: suhendi@telkomuniversity.ac.id

© 2026 IISTR

operating point approaches the maximum [6]. This control concept provides a basis for investigating the application of P&O to oxygen concentrator systems.

The performance of a PSA oxygen concentrator is also strongly influenced by the adsorbent properties and operating conditions. Li-X zeolite with a particle size of 0.4 mm has been reported to provide higher oxygen purity than 13X zeolite and other particle sizes [11]–[12]. An adsorbent volume equivalent to approximately 90% of the chamber volume has also been reported to improve oxygen purity [11]. In addition, adsorption time and pressure affect the adsorption performance of zeolite [4], [13]. These findings indicate that appropriate control of PSA operating conditions is essential for improving oxygen concentration and system efficiency.

B. Oxygen Concentrator

As the word "concentrator" indicates the concentration or enrichment of anything, and here oxygen is being concentrated from the air mixture. So, in layman's language, we can say that this device concentrates oxygen from the air by eliminating nitrogen from them [7]. Metal cylinders designed to hold high-pressure compressed gases are called oxygen cylinders [2]. The oxygen concentrators are constructed using several parts, including a flow splitter, an air inlet, a waste exit, filters, and a control. The oxygen cock, valve, and power switch make up the control. In addition, it contains a filter, product canister, pressure regulator, zeolitized sieve canisters, compressor, and solenoid-controlled valve [7].

By removing nitrogen from the air, oxygen concentrators may produce nearly pure oxygen from ambient air, which typically comprises 21% oxygen, 78% nitrogen, and 1% other gases. Unlike compressed or liquid oxygen tanks that need refilling, an oxygen concentrator continuously purifies the atmospheric air to deliver oxygen directly to patients. They offer an oxygen supply that is safer, more affordable, dependable, and more economical than oxygen cylinders, especially in environments with limited resources [8].

C. Pressure Swing Adsorption

The technology is referred to as pressure swing adsorption because the air pressure fluctuates between the two containers. Selective adsorption of nitrogen can improve the efficiency of both oxygen synthesis and oxygen recovery in a pressure swing adsorption (PSA) method for producing oxygen from ambient air [7]. PSA relies on the high-pressure adsorption of gases. The volume of gas that is adsorbed increases with increasing pressure. Typical components of an oxygen generating plant include an air compressor, a reservoir, controls, a dryer, filters, and two separation chambers [2]. This device uses ambient air in a highly pressurized tank to separate the many gases that are found in the atmosphere. The zeolites in the tank produce dipoles when pressure is applied to them. Nitrogen gas is collected, and oxygen gas is separated in the tank due to the dipole that the chosen zeolite creates. After some time, the maximum amount of nitrogen adsorption causes zeolite to become saturated. In order to regenerate zeolite, the tank's pressure is lowered to atmospheric pressure, allowing nitrogen to be released and the zeolite to revert to its original polarity [14].

The pressure of the feed gas determines the high pressure at which impurity adsorption occurs. The direction of the feed gas flow through the adsorber vessels is upward. Nitrogen and other impurities are specifically adsorbed on the adsorbent material's surface. At the top of the adsorber tank, highly pure products emerge. The adsorption phase ends, and regeneration begins after a predetermined amount of time. To guarantee a steady supply of goods, another adsorber assumes responsibility for the adsorption process. To stop impurities from penetrating the top of the adsorber, the residual pressure must eventually be discharged in a countercurrent direction. This is the initial stage of the regeneration phase, during which desorbed contaminants enter the PSA plants exhaust gas system from the adsorber at the bottom [15].

The adsorption tanks are loaded alternately to ensure a steady flow of product. When one adsorption tank is filled, the other is simultaneously renewed through desorption, or a drop in pressure. All it takes to achieve the depressurization needed for regeneration is to simply vent to the atmosphere. Pressure equalization between the adsorption vessels will occur before the ensuing adsorption and desorption phase, to preload the regenerated vessel with a gas high in product [16].

D. Perturb and Observe Algorithm

The Perturb and Observe method is widely utilized in MPPT PV controllers because of its simplicity and convenience of use. Two sensors measure the solar panels' output voltage and current, from which the output power is calculated. If the power increases, all that must be done is to keep the voltage change going in the same direction. If not, change the voltage in the opposite direction from the one that was initially applied. After a stable state is achieved, the algorithm swings around the peak power point [17]. The P&O algorithm compares the most recent result with the prior one and chooses the best one using this technique, then moves on to monitor MPP after giving these initial values to the variables voltage, current, and power. The P&O method modifies the duty cycle of the voltage in the second step, and then it compares the power change to the initial reading. If the change is positive, the disturbance will persist until the power change due to the voltage change turns negative. The P&O has crossed the MPP, as indicated by the negative change. Therefore, the P&O algorithm begins toggling around the MPP when it detects a decrease in power, at which point it reverses the direction of perturbation and goes back towards the MPP [18].

Traditional algorithms are easily designed and programmable, and they can track the MPP efficiently. However, because a PV cell's characteristic curve has numerous peaks that arise, they are vulnerable to situations where there is partial shade. Conventional algorithms' search methodology prevents them from locating the genuine or Global MPP (GMPP) among all the other local peaks. The optimal duty cycle is selected by the strategic P&O algorithm to resolve this issue [6].

The operating method involves bringing the operational power point closer to MPP with a large step size. The strategic P&O moves the operational point in the other direction until it detects another MPP cross. The step size is then decreased by two. It selects MPP as the final output after the second cross and steps down by four for the first time. The moment

the power change is detected, the strategic P&O algorithm begins to operate. Achieve an open-circuit voltage at the operational point before starting the first duty cycle change for just the first iteration. After then, it continues to move in the same general direction toward MPP, stepping heavily, until it reaches the first MPP crossing. The tracking direction of the strategic P&O approach is reversed with a step size that is half of the initial step size, and it propagates farther until it detects a second cross. After the second cross to the MPP with one-fourth of the initial step size, the strategic P&O algorithm moves in the opposite direction to produce a steady and oscillation-free output [6].

E. Zeolite as Adsorbent

The best mineral for separating oxygen is zeolite, which does so by mainly adsorbing nitrogen. This effectiveness results from the complex three-dimensional hexagonal honeycomb structure of the zeolite, which is endowed with a net negative charge and forms a cage-like structure that is effective at ensnaring nitrogen molecules. Because nitrogen has a greater quadrupole moment, which controls the nuclear charge distribution and gas molecule structure, it selectively adsorbs onto the zeolite surface [12]. With additional skeletal zeolite cations, N_2 molecules exhibit a stronger electrostatic attraction because of their higher quadrupole moment compared to O_2 molecules. Therefore, the differential in electrostatic attraction between the adsorbate molecule and the adsorbent surface accounts for nitrogen's selectivity towards oxygen. This electrostatic interaction for adsorbed N_2 molecules with a greater quadrupole moment (about three times higher than O_2 molecules) with smaller non-skeletal Li+ cations swapped with much larger Li+ cations occurred in 13X zeolite traded for Li+. Increased selectivity for the adsorption of nitrogen gas from air is correlated with a higher charge density, as indicated by the charge/radius ratio [19].

The absorption performance of gas by zeolite is also influenced by several factors, including the size of the zeolite, air pressure, temperature, and the concentration of the adsorbent. Zeolites with larger porous sizes tend to have a higher absorption capacity because they allow more nitrogen molecules to enter. At higher pressure, more molecules of nitrogen can be absorbed by zeolite. Lower temperatures usually increase the absorptive capacity of nitrogen. The concentration of nitrogen in the air also affects the absorption performance [3]. The relationship between nitrogen adsorption by zeolite and pressure can be described using adsorption isotherm models. Among the commonly used models, the Langmuir isotherm in equation (1) provides a useful approach for describing the equilibrium adsorption behavior of nitrogen on zeolite.

$$q_e = \frac{q_m K P}{1+KP} \quad (1)$$

Where q_e is the amount of nitrogen adsorbed per unit mass of zeolite (mmol/g), q_m is the maximum adsorption capacity of the zeolite (mmol/g), K is the Langmuir adsorption equilibrium constant (Pa^{-1}), and P is the equilibrium pressure of nitrogen (Pa). This equation shows that at low pressure, adsorption increases linearly with pressure, but at high pressure, the adsorption reaches a maximum value that cannot be exceeded. When zeolite is no longer able to adsorb, the unabsorbed adsorbates will be remixed with other gases [13].

III. METHODOLOGY

A. System Design

Fig. 1 shows the general architecture of the system. The air source section, the process section, and the outcomes section are the fundamental parts of the system. The partition of this section can be marked with a blue dashed line shape. The compressor, which supplies compressed air, and the air filter regulator, which filters unwanted particulates carried by the compressor's air flow. During the experiment, the compressor worked non-stop which resulted in an increase in humidity in the air pushed by the compressor. This moisture affects the performance of nitrogen absorption by zeolite, where the element H_2O will cover the surface of the zeolite thereby blocking nitrogen from being absorbed. These are in the air source section.

The next section is the process section, which has two chambers for the adsorption process. These chambers are going to be filled with Li-X 0.4mm zeolite adsorbents with a total of 90% of the chamber volume [11]. In addition, a pressure sensor is used to measure the pressure inside the chamber, and a solenoid valve operates as a gate to allow air to enter or dissipate the chamber. The air that has been held in the chamber will be expelled through two paths. Namely nitrogen gas that is exhausted to the free air, and also oxygen products that are distributed to the next section.

The final section is the output section, where high-oxygen pure air is circulated. Following the process of adsorption within the chamber, oxygen is transferred to a storage area. The oxygen sensor measures the amount of oxygen flowing along the path. However, before the air flow reaches the oxygen sensor, it flows through a pressure regulator, which reduces the flow pressure in accordance with the sensor's measuring capabilities.

The chamber, which provides the setting or space for the adsorption process, and the Li-X zeolite container are the main components of the required hardware. The dimensions of this chamber in height 25cm, inner diameter 8cm, fitting diameter ¼ inch, and material thickness 5mm. To keep the zeolite from being pulled out by airflow, each of these holes has a wire mesh filter with a size of 100.

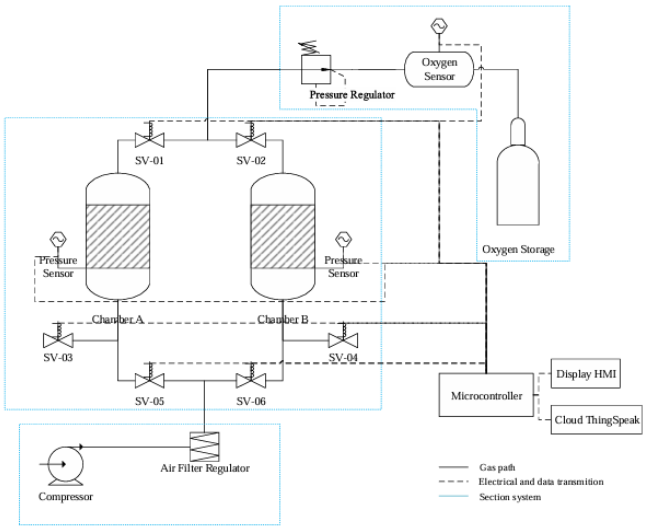


Fig. 1. System Design

The electricity in this system is marked by a black dash line where the component is controlled by a microcontroller.

These components are pressure sensors and oxygen sensors whose values will be read, and actuators in the form of solenoid valves with on-off controls. The readings from the pressure sensor and oxygen sensor are processed by a microcontroller, the processed data is displayed on the human machine interface (HMI) display and also sent to the ThingSpeak cloud which can later be viewed visually through an android-based application. The components used are six solenoid valves AirTAC 2V-025-08 that function as gate airflow according to the path and fittings in the system. Chip relay ULN2003 is used to disconnect or connect the coil to the solenoid valve, controlled by Arduino uno. This solenoid valve requires 12 volts of power, while for other components it only requires 5 volts. The reading sensor has been modified to match the state of the system. Such as pressure sensors WNK83N010Z used with a reading range of 0-10 bar with output voltage 0.5-4.5 volt, therefore calibration must be carried out. The oxygen sensors KE-25 can measure an oxygen concentration range of 0–100% with an output voltage of just 0-65 millivolts. Because the oxygen sensor voltage output was inappropriate, the oxygen sensor amplifier circuit was designed with a gain of 70x in order to match the Arduino reading capabilities. For system monitoring needs, human machine interface Nextion displays are used as display on equipment, and ESP32 used as a device that transmits data to the IoT platform ThingSpeak.

B. Workflow System

The basic program flow of the system starts with initialization of the pins of the digital relay solenoid valve being turned on and off, and variables. According to the PSA procedure for each scenario, the pin digital relay solenoid valve has been programmed to be controlled in each case. Followed by pressure and oxygen sensors readings. After that, the process is carried out according to which scenarios are running. Explanations of each scenario will be discussed next. The data that obtained is delivered to ESP32 every second to be transmitted to the ThingSpeak platform to be processed and displayed to users in Android-based mobile applications, and the information is also shown on the HMI display.

PSA methods are performed for all scenarios, where there is still rising and falling pressure on the chamber. In whole scenarios, the controls are based on time scheduling. Where the time that will be set is the length of time each solenoid valve is opened and closed according to the function and purpose of the running scenario.

C. P&O Algorithm

For the P&O function part, it can be seen in Fig. 3 starting by defining and updating the variables used in P&O such as the step variable which is the D value for the time update added to the next cycle time, then t as an iteration variable where each cycle is carried out, the O variable is the oxygen sensor reading, and T is cycle time. The workflow of this algorithm is when the average value of the current oxygen concentration is greater than before and the current cycle time is larger than before, then the next cycling time is added by the step time.

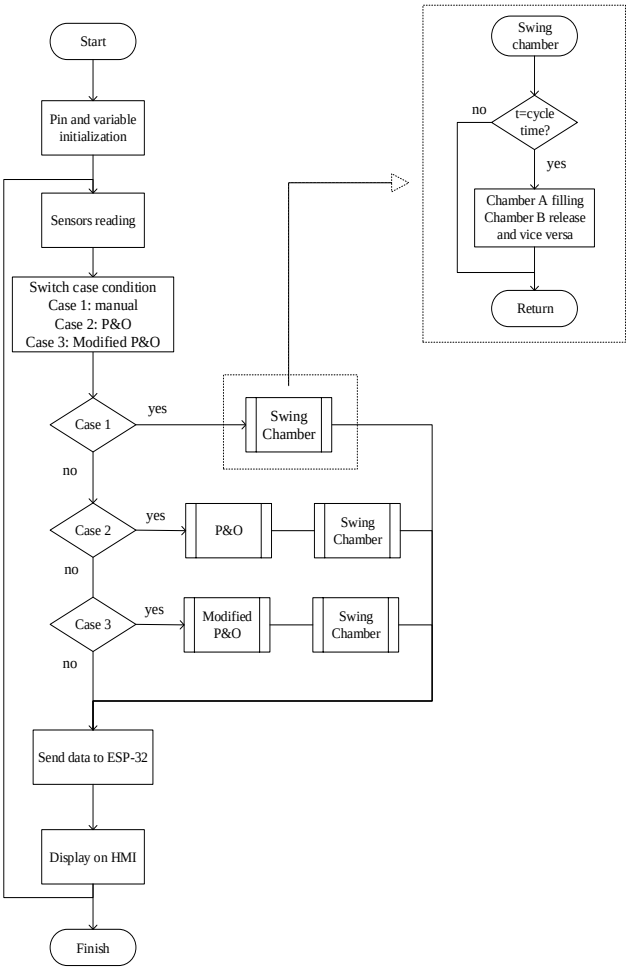


Fig. 2. Workflow System

However, if the present cycle times are smaller than before then the following cycle time is reduced by the step. This applies in reverse if the current average oxygen concentration values are lower than before. Cycle time changes and other variable updates are done after iteration reaches 300, if it has not reached that, the PSA cycle method will continue to be done with the same cycle time. The experiment will stop when it has reached its peak, this can be seen when the cycle-time changes flow back and forth on one range of cycle times are the same for several crossing times.

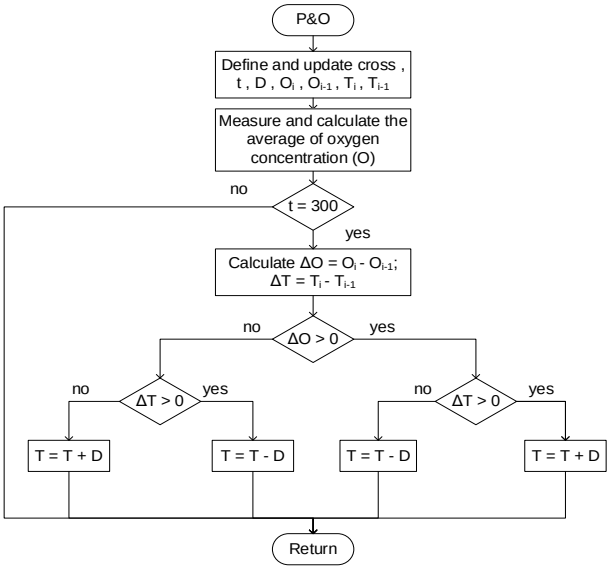


Fig. 3. Flowchart of Perturb and Observe Algorithm

D. Modified P&O Algorithm

In line with the problem already written in the previous subchapter that the weakness of the P&O algorithm is the looping process because it finds the maximum local point, while there is a possibility that the actual maximum global point is on the right side of the graph or on the next process. Then from that, modified step size needed [8]. In this research modified P&O was applied where the step value at the beginning of the cycle was made bigger, which was four seconds. Then if a crossing is identified in the P&O pattern, the step value will be divided by two. This crossing is identified if there is a deviation from the previous pattern, seen from the occurrence of a decrease in the average concentration of oxygen that the next process will reverse the direction of the pattern.

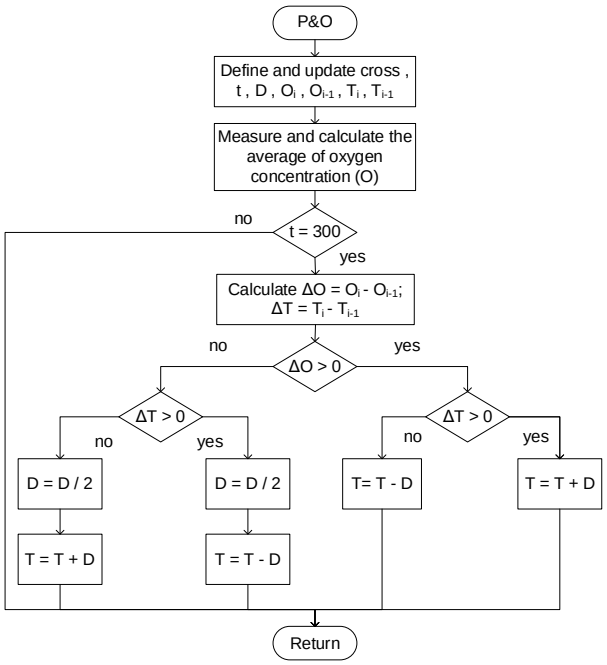


Fig. 4. Flowchart of Modified Perturb and Observe Algorithm

E. PSA Procedure

The scheme of each solenoid valve can be seen in Fig. 5. The SV-01 and SV-02 are located on the oxygen release output line at each chamber, SV-03 and SV-04 are located at the nitrogen release output line at each chamber, and SV-05 and SV-06 are on the air supply inlet line at each chamber.

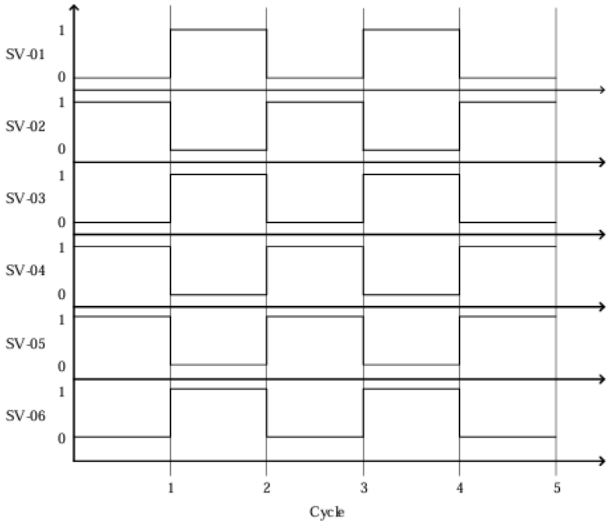


Fig. 5. Swing Chamber Scheme

The swing chamber determines the optimal pressure for this system by opening the intake air path, and closing the oxygen and nitrogen releases path at the same time. After that, the intake air path is closed, and opens the oxygen and nitrogen release path. In the other words, opening the left inlet chamber valve and releasing oxygen and nitrogen outlets in the right chamber. This process is repeated repeatedly until sufficient data is collected.

IV. Experiments and Discussion

A. System Profile

Some sensors and actuators in this system require additional components in order to process measurements or actions. The signal from the Arduino digital pin is connected to the solenoid valve's coil through the ULN2003AN integrated circuit working as a relay or switch. Furthermore, resistors according to the appropriate gain value are present, along with two LM358 ICs used as op-amps. The KE-25 oxygen sensor's value is gained using amplifier circuits so that an analog Arduino pin can read it.

In order to protect some components from external influences and reduce the possibility of interference during the reading process, they are placed inside a 125x175x100 mm^3 panel box. The box contains a few other parts besides the PCB, including the display HMI Nextion, Arduino Uno, ESP32 module, and cable connectors. Some parts, such as the sensors and actuators, are located closer to the chambers.

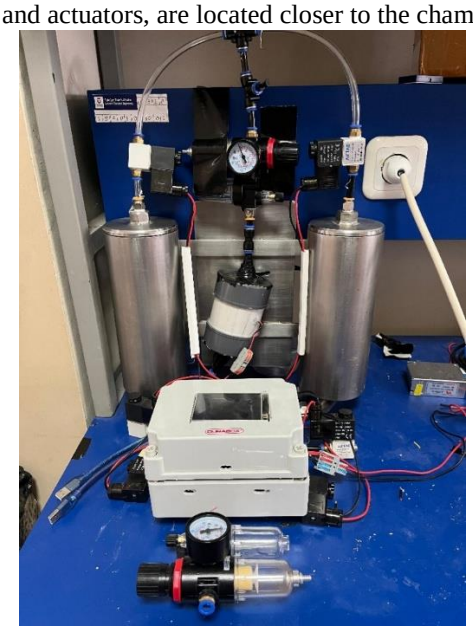


Fig. 6. Setup of Oxygen Concentrator System

A 24-liter compressor is used to compress air into a chamber with an air output rate of about 29 liters per minute. Each of the two chambers dimensions 25 cm in height and 8 cm in diameter. The material used to construct this chamber is 5 mm thick stainless steel 304. Inside the chamber, Li-X zeolite is added with a diameter of 0.4mm as much as 90% of the chamber volume. A higher concentration of oxygen-containing air flows toward the oxygen storage, which was previously measured by the oxygen sensor, once the chambers adsorption operation is finished.

The chamber is supplied with air from the compressor gradually from low pressure and increases with the condition of the outlet path closed. The purpose of this test is to verify that the chamber can handle the conditions of a compressor

that is fully opened. Following the test, the chamber is capable of withstanding 6.40 bar of compressor air for the left chamber and 6.79 bar for the right chamber without having any leakage. In addition, the same method is used to verify the connections flowing from the chamber, including the inlets and outlets. If there's leaking, maintain tightening the chamber's connection until there are none at all.

B. Sensor Calibration

Calibration is carried out to obtain the equation of the relationship between the value emitted by the oxygen sensor KE-25 and the value of the actual oxygen concentration. The true oxygen concentration value is obtained from the oxygen analyzer CY-12C reading. Both are attached to a tube, which is then filled with oxygen of high purity slowly so that several points of concentration value are obtained. From the results of the calibration with linear regression, it is known that the equality between bytes and oxygen concentration is:

$$y = 0.1264x + 4.45348 \quad (2)$$

With y representing oxygen concentration (%), and x is the output bytes of the sensor. This equation will be inserted into the program in the Arduino so that it can calculate the appropriate physis value.

The validating was done in the same pattern as the calibration. The difference is the parameters that will be compared are the oxygen concentration values read on an oxygen analyzer with those read on an Arduino. The oxygen sensor validation resulted in an average error of 1.24%.

Similar to the calibration and validation steps on the oxygen sensor, for calibration of pressure sensors, compared sensor readings with pressure gauge reading values. Both are attached to the chamber which will then be input air using a compressor in the chamber slowly with the output path closed, resulting in several pressure points. The pressure sensor on the left and right chambers produces the calibrating result equations of (3) and (4) respectively as follows:

$$y = 0.0118x - 1.1687 \quad (3)$$
$$y = 0.012x - 1.1498 \quad (4)$$

With y representing oxygen concentration (%), and x is the output bytes of the sensor. The pressure sensor on the left chamber validation resulted in an average error of 1.41%. The pressure sensor on the left chamber validation resulted in an average error of 1.61%.

C. Manual Experiment

The manual experiment was carried out in stages with a step cycle time of two seconds. Every time the cycle time changes, the process is stopped first to update the source code on the microcontroller. This experiment was carried out up to a cycle time of 18 seconds, where it was observed that the pattern of oxygen concentration decreases after a cycle time of eight seconds. This decrease in oxygen concentration is caused by a pressure difference in the chamber. The pressure in the chamber affects the performance of zeolite in adsorbing nitrogen.

The pressure behavior in the two chambers at a cycle time of eight seconds performs a pressure swing with an average upper pressure of 2.8 bar and an average bottom pressure of 0.86 bar. The pressure immediately increases when the chamber is filled and immediately decreases when oxygen and nitrogen are released.

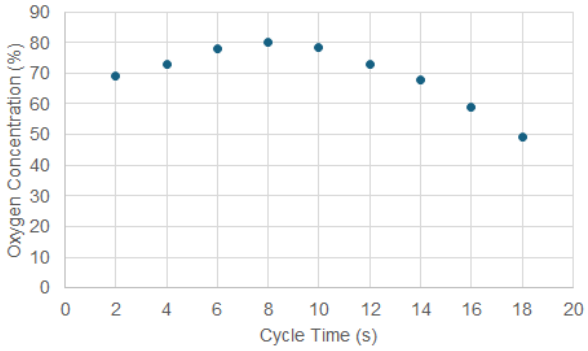


Fig. 7. Cycle Time Comparison of Manual Experiment

Fig. 7 shows the relationship between cycle time in seconds (s) and oxygen concentration in percentages (%). The x axis represents the time of the cycle while the y axis shows the oxygen concentration. The graph shows a trend of decreasing oxygen concentration as cycle time increases. This shows that over time the pressure in the chamber has increased as in Fig. 8. According to (1), the performance of oxygen nitrogen absorption depends on pressure, and this causes the concentration of the oxygen produced by the system to decrease.

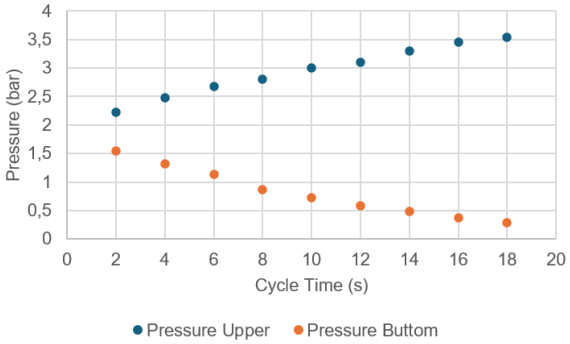


Fig. 8. Pressure Result of Manual Experiment

From the manual experimental data, the optimal cycle time with the highest oxygen concentration was obtained, namely with a cycle time of eight seconds. After obtaining data from the results of the experiment by manual update, curve fitting is carried out which will later become reference data for experiments with the P&O algorithm. Curve fitting is done on MATLAB software with custom equation mode. The resulting ratio of a:b is 1:16 with the value of C calculated automatically on the MATLAB. The fitting formula obtained is as follows:

$$O = -0.3586T^2 + 5.7376T + 57.37 \quad (2)$$

with O presents oxygen concentration, and T is cycle time.

After the data collection is done manually and the curve fitting is performed, the data is met, with the aim of being the reference value for experiment by applying the perturb and observe algorithm and also modifying it.

D. P&O and Modified Experiment

Graphs in Fig. 9 and Fig. 10 show the relationship between cycle time in seconds (s) and oxygen concentration in percentages (%). The x-axis represents the time of the cycle, while the y-axis shows the oxygen concentration. The experiment using the P&O method yielded the following

results, which are shown in Fig. 9. The step size used throughout the process remains at two seconds. A drop in oxygen concentration causes the pole's orientation to shift, causing crossing to happen at a cycle time of ten seconds and five seconds at the second crossing. The oxygen concentration is highest when the cycle time is eight seconds.

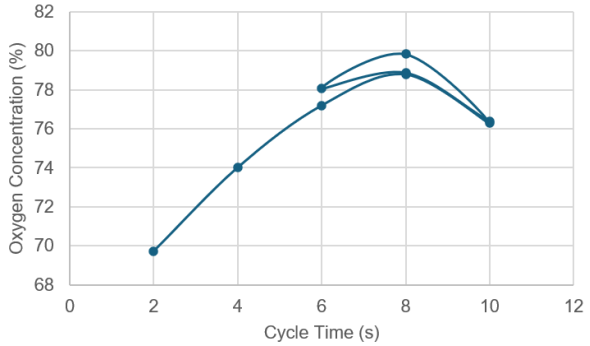


Fig. 9. Cycle Time Comparison with Perturb and Observe Algorithm

An experiment with the modified P&O algorithm was carried out starting with a large step cycle time of four seconds; then a crossing occurred that reduced the step to two seconds, and it happened again until the step was only one second. The first crossing occurred at a cycle time of twelve seconds, then stepped to two seconds and a crossing occurred again at the second six-second cycle time. The step was updated back to one second, and the highest oxygen concentration value was obtained at a cycle time of eight seconds.

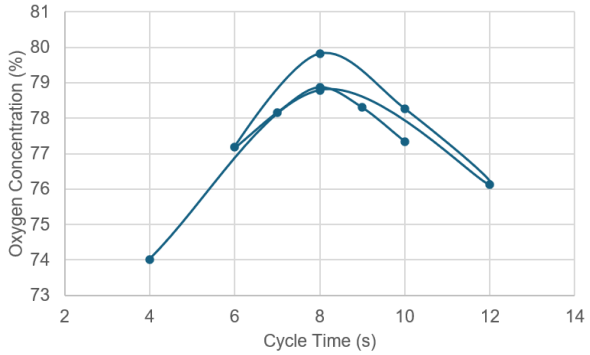


Fig. 10. Cycle Time Comparison with Modified Perturb and Observe Algorithm

From experiments with the P&O algorithm as well as with the modified P&O algorithm, optimum cycle time values were obtained which resulted in the highest oxygen concentration at the value of eight seconds. This value is also the same as in a manual test which also has an optimal cycle time of eight seconds.

E. Comparison

Both Fig. 11 and Fig. 12 are comparisons of the oxygen concentration obtained by the P&O algorithm and the modified P&O algorithm against the manual experiment data. The data point selected from the P&O algorithm experiment and its modification is the outermost point of all available data because of the layers of the crossing path for the oxygen concentration. The optimal cycle time for both is eight seconds to get the highest oxygen concentration. The average error percentage resulting from the two comparisons above was 1.23% and 1.36%.

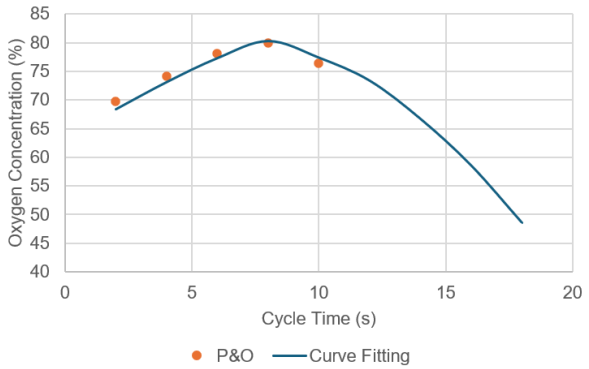


Fig. 11. Comparison Between P&O and Manual Experiment

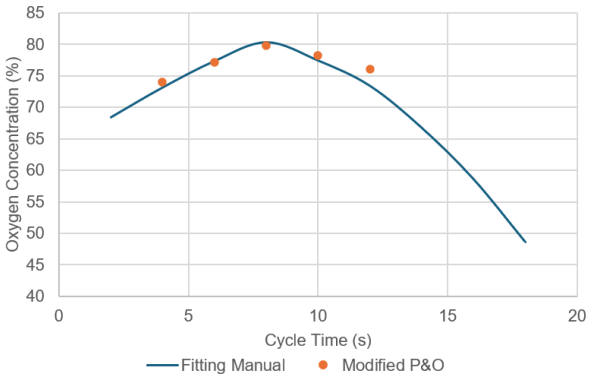


Fig. 12. Comparison Between Modified P&O and Manual Experiment

Fig. 13 and Fig. 14 are comparisons of the oxygen concentration obtained from the P&O algorithm and modified P&O algorithm experiments with the curve-fitting results from the manual experiment. The optimal cycle time of both is eight seconds to get the highest oxygen concentration. From the distribution of the data above, the average error percentage of both comparisons was 1.75% and 1.28%.

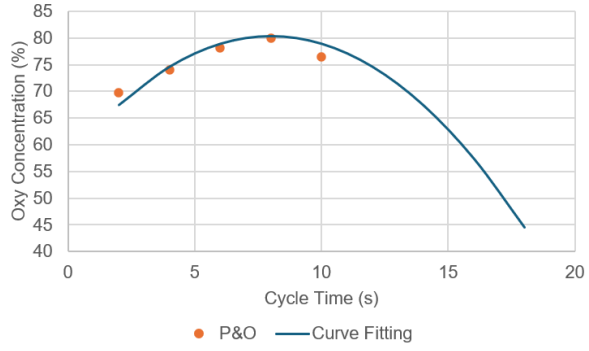


Fig. 13. Comparison Between P&O and Curve Fitting

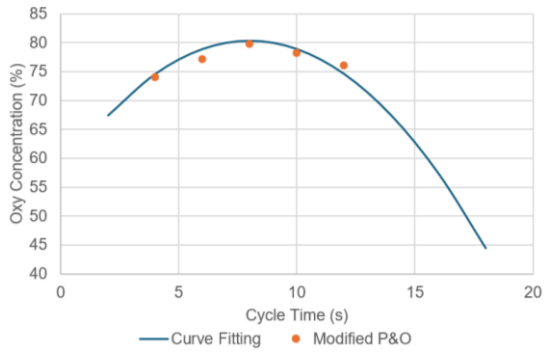


Fig. 14. Comparison Between Modified P&O and Curve Fitting

V. CONCLUSION

This research developed a prototype oxygen concentrator based on pressure swing adsorption (PSA) with an automated Perturb and Observe (P&O) algorithm for determining the cycle time that produces the highest oxygen concentration. The system uses 0.4 mm Li-X zeolite in two stainless-steel adsorption chambers and integrates pressure and oxygen sensors with an automated solenoid-valve control system. The conventional P&O algorithm and the proposed modified P&O algorithm were evaluated against manual experiments.

The experimental results show that both P&O approaches identified an optimal cycle time of 8 s, corresponding to a maximum measured oxygen concentration of 80.32%. The conventional P&O algorithm produced an average error of 1.23% when compared with the manual experimental data and 1.75% when compared with the curve-fitting results. The modified P&O algorithm produced average errors of 1.36% and 1.28%, respectively. The modification, which starts with a larger step size of 4 s and reduces the step size after detecting a crossing point, enabled the algorithm to search for the optimum cycle time without requiring the system to be stopped during the optimization process.

The current results are limited to the prototype configuration and the laboratory operating conditions used in this study, including the specific chamber dimensions, Li-X zeolite loading, compressor capacity, and tested cycle-time range. Therefore, the results should not yet be considered representative of all oxygen concentrator operating conditions or full-scale medical applications. Future work should investigate the performance of the modified P&O algorithm under a wider range of operating pressures, flow rates, environmental conditions, and adsorbent conditions, as well as evaluate long-term system stability and scalability toward practical oxygen concentrator applications.

REFERENCES

[1] N. S. Pravda, M. S. Pravda, R. Kornowski, and K. Orvin, "Extracorporeal membrane oxygenation therapy in the COVID-19 pandemic," *Future Cardiology*, vol. 16, no. 6, pp. 543-546, 2020, doi: 10.2217/fca-2020-0040.

[2] N. Bhat, V. Moses, and C. N., "Economical synthesis of oxygen to combat the COVID-19 pandemic," *Hygiene and Environ. Health Adv.*, vol. 6, e100048, 2023, doi: 10.1016/j.heha.2023.100048

[3] C. Chin, Z. Kamin, Mohd H. V. Bahrun, and A. Bono, "The production of industrial-grade oxygen from air by pressure swing adsorption," *Int. J. Chemical Eng.*, vol. 2023, no. 1, e2308227, 2023, doi: 10.1155/2023/2308227.

[4] Q. Liu, R. Xiang, Y. Zhai, and L. Cui, "Exploration of the adsorption and desorption performance of volatile organic compounds by activated carbon with different shapes based on fixed-bed experiments," *Chemosphere*, vol. 364, e143161, 2024, doi: 10.1016/j.chemosphere.2024.143161.

[5] X. Zhu, Y. Liu, X. Yang, and W. Liu, "Study of a novel rapid vacuum pressure swing adsorption process with intermediate gas pressurization for producing oxygen," *Adsorption*, vol. 23, pp. 175–184, 2017, doi: 10.1007/s10450-016-9843-4.

[6] M. M. Afzal, "Strategic perturb and observe algorithm for partial shading conditions: SP&O algorithm for PSC," *Sir Syed Univ. Res. J. Eng. Technol.*, vol. 12, pp. 26–32, 2022, doi: 10.33317/ssurj.497.

[7] T. A. Madankar and Y. Deshpande, "Development of portable oxygen concentrator—A review," *E3S Web of Conf.*, vol. 430, e01265, 2023, doi: 10.1051/e3sconf/202343001265.

[8] G. A. Prayoga, E. Husni, and S. D. Jaya, "Design of an embedded controller and optimal algorithm of PSA for a novel medical oxygen concentrator," *Int. J. Electr. Eng. Inf.*, vol. 15, no. 2, pp. 220–239, 2023, doi: 10.15676/ijeei.2023.15.2.4.

[9] S. Singhal et al., "Engineering aspects on the design and realization of medical oxygen concentrator for oxygen therapy," in *E. Chinthapudi, S. Basu, and B. N. Thorat (eds) Sustainable Chemical, Mineral and Material Processing*, Lecture Notes in Mechanical Engineering, 2022, doi: 10.1007/978-981-19-7264-5_2.

[10] G. Mamatha, "Perturb and observe MPPT algorithm implementation for PV applications," *Int. J. Comput. Sci. Inf. Technol.*, vol. 6, pp. 1884–1887, 2015. [Online]. Available: https://www.ijcsit.com/~ijcsitco/docs/Volume%206/vol6issue02/ijcsit20150602216.pdf

[11] S. N. Hida, A. N. Putra, M. Y. Nurjaya, M. B. Sunaryo, and A. Suhendi, "The effect of adsorbent-material properties on PSA based oxygen concentrators," in *Proc. 4th Eng. Physics Int. Conference, Bandung, Indonesia*, vol. 2673, e012035, 2023, doi: 10.1088/1742-6596/2673/1/012035.

[12] S. Shrivastava, A. Verma, J. Ramkumar, and R. Aryal, "A comprehensive study for improving the working parameters for the design of a PSA-based oxygen concentrator," *Eng. Res. Express*, vol. 6, 2024, doi: 10.1088/2631-8695/ad1215.

[13] Y. Wang et al., "High pressure excess isotherms for adsorption of oxygen and nitrogen in zeolites," *Langmuir*, vol. 27, no. 17, pp. 10648–10656, 2011, doi: 10.1021/la201690x.

[14] H. Aljaghoub et al., "Comparative analysis of various oxygen production techniques using multi-criteria decision-making methods," *Int. J. Thermofluids*, vol. 17, e100261, 2023, doi: 10.1016/j.ijft.2022.100261.

[15] Hydrogen Recovery by Pressure Swing Adsorption, Canada: The Linde Group. [Online]. Available: https://assets.linde.com/-/media/global/engineering/engineering/home/products-and-services/process-plants/adsorption-and-membrane-plants/hydrogen-recovery-and-purification/ha_h_1_1_e_09_150dpi_nb.pdf

[16] A. D. Wiheeb, Z. Helwani, J. Kim, and M. R. Othman, "Pressure swing adsorption technologies for carbon dioxide capture," *Separation & Purification Rev.*, vol. 45, no. 2, 2016, doi: 10.1080/15422119.2015.1047958

[17] A. Harrag and S. Messalti, "Variable step size modified P&O MPPT algorithm using GA-based hybrid offline/online PID controller," *Renewable and Sustain. Energy Rev.*, vol. 49, pp. 1247–1260, 2015, doi: 10.1016/j.rser.2015.05.003.

[18] A. Ibrahim, R. Aboelsaud, and S. Obukhov, "Improved particle swarm optimization for global maximum power point tracking of partially shaded PV array," *Electr. Eng.*, pp. 443–455, 2019, doi: 10.1007/s00202-019-00794-w.

[19] A. Das and A. K. Das, "Quadrupolar interaction with zeolite and pressure swing adsorption in portable medical oxygen concentrators for breathing of COVID-19 and COPD patients," *Resonance*, vol. 27, no. 8, pp. 1387–1409, 2022. [Online]. Available: https://www.ias.ac.in/public/Volumes/reso/027/08/1387-1409.pdf



Shalma Nur Hida received a Bachelor's degree in Engineering in 2022. She is fresh graduated the Master degree of Engineering with the School of Electrical Engineering, Telkom University, Bandung, Indonesia. Her research interests include electrical instruments and control systems. (email: shalmahida@telkomuniversity.ac.id).



Asep Suhendi received the Bachelor and Master degrees of Science from Bandung Institute of Technology, Bandung, Indonesia, in 2005 and 2008. He received the Doctoral Degree in Chemical Engineering in 2013 from Hiroshima University, Japan. In his academic career, he has made significant contributions as a Lecturer and as Deputy Director at PUI-PT. His dedication to research can be seen from his publications, showing a productive and respected scientific track record with an h-index of 6 and an i10-index of 29. His research interests include instrumentation, physics, physical engineering, aerosols, nanomaterials, chemical engineering, and electrical engineering. (email: suhendi@telkomuniversity.ac.id).



Muhammad Zakiyullah Romdlony received the bachelor's and master's degrees in electrical engineering from Bandung Institute of Technology, Bandung, Indonesia, in 2009 and 2012, respectively, and a Ph.D. degree in System and Control in 2018 from the University of Groningen, the Netherlands. Currently, he is the head of the expertise group of Control Electronics and Intelligent Systems at the School of Electrical Engineering, Telkom University, Indonesia. His research interests include nonlinear control systems, robust control, and robotics. (email: zakiyullah@telkomuniversity.ac.id).